

Ashraf Hamid<sup>1</sup>, Hesham Shahbunder<sup>2</sup><sup>1</sup> Department of Radioactive Environmental Pollution, Hot Laboratories Center, Atomic Energy Authority, Cairo, Egypt<sup>2</sup> Physics Department, Faculty of Science, Ain Shams University, Cairo, Egypt**k<sub>0</sub>-PGNAA OF POLLUTANTS IN AQUEOUS SAMPLES USING MCNP CODE**

Prompt  $\gamma$ -neutron activation analysis (PGNAA) using the  $k_0$  method by employing the 1951.1 keV  $\gamma$ -line of the  $^{35}\text{Cl}(n, \gamma)^{36}\text{Cl}$  thermal neutron reaction as monostandard comparator was described. The method has been applied and evaluated using the anti-Compton prompt  $\gamma$ -ray neutron activation analysis facility using  $^{252}\text{Cf}$  neutron source with a neutron flux of  $6.16 \cdot 10^6 \text{ n} \cdot \text{cm}^{-2} \cdot \text{s}^{-1}$ . A well-type HPGe detector as the main detector surrounded by NaI(Tl) guard detector has been arranged to investigate the performance of the Compton suppression spectrometer using the simplified slow circuit. The properties of neutron flux were determined by MCNP code calculations. In order to determine the efficiency curve of an HPGe detector, the prompt  $\gamma$ -rays from chlorine were used and an exponential curve was fitted. AC-PGNAA method has been used for the determination of high neutron absorbing elements like Cd, Sm and Gd as well as 20 light and heavy elements (Na, Mg, Al, Si, P, K, Ca, Ti, V, Mn, Sc, Fe, Co, Zn, La, Rb, Cs, As and Th) in standard reference materials (IAEA, Soil-7) and ten sediment samples collected from El-Manzala lake in northern part of Egypt. The reference material IAEA, Soil-7 was analyzed for data validation and good agreement between the experimental values and the certified values have been obtained.

*Keyword:*  $k_0$ -PGNAA, AC-PGNAA,  $^{252}\text{Cf}$  neutron source, water pollution, MCNP code, self shielding.

**Introduction**

Neutron induced prompt  $\gamma$ -ray activation analysis (PGAA) is based on the observation of instantaneous  $\gamma$ -radiation following the neutron reaction, which is mostly radiative capture, usually denoted as  $(n, \gamma)$  reaction. The energies of the emitted  $\gamma$ -rays are characteristics of the element (more precisely, it's radiating isotope), whereas the corresponding spectral intensities are proportional to the elemental content. PGAA is a rapidly developing technique, pursued with intense reactor beams as well as portable neutron sources. It is applicable to all elements including the light elements, which are usually difficult or even impossible to measure in neutron activation analysis (NAA) utilizing radioactive decay  $\gamma$ -rays. Moreover, for certain nuclides PGAA provides substantially higher sensitivities. Further advantages are its non-destructive nature due to the substantially lower neutron flux, the lack of sample preparation needs, and the ability to obtain results promptly [1]. A major obstacle to the use of the PGAA method for quantitative multi-element analysis has so far been the absence of a high-quality database of characteristic prompt  $\gamma$ -ray energies and intensities. In a prompt spectrum, the very large number of peaks (order of 1000) tremendously increases the chance for spectral interference [2].

Because the escaping energy is a photon, it is possible to collect that energy with another detector. This is typically done with a larger detector made of a less expensive material such NaI(Tl) surrounding

the main detector, and is known as a surrounding shield "guard". By correlating events in the main detector and the surrounding shield detector with timing electronics, events counted in the shield detector can be used to reject simultaneous events in the main detector (veto signal). Therefore, a veto action is made to discard the signal from being counted as a true data. This results in the suppression of the Compton continuum which results in removing the Compton-associated background, therefore, enhancing the signal-to-noise ratio and improving the detection capability of the system [3].

In the present work, the  $k_0$ -PGNAA has been applied to the analysis of major and trace elements of sediment samples collected from the Manzala Lake in northern parts of Egypt, as well as a careful and complete characterization of the neutron flux parameters in the selected irradiation positions.

**Theory****Internal Single Comparator (monostandard) Method ( $k_0$ -PGAA Method) [4]**

The usual analysis for PGAA was carried out using a comparative method. Indeed, element concentrations (or masses) were determined by comparing the specific  $\gamma$ -ray count rate ( $A_{sp}$ ), usually given in  $(\text{counts} \cdot \text{s}^{-1} \cdot \text{g}^{-1})$  units of an element in an unknown sample to the corresponding element. The relevant k-factor is easily obtained as a ratio of specific count rates for sample x and comparator or rather its simplified form [4]:

$$K_c(x) = \frac{A_{sp,x}}{A_{sp,c}} = \frac{(\theta\sigma I/M)_x \cdot \epsilon_x}{(\theta\sigma I/M)_c \cdot \epsilon_c}, \quad (1)$$

where

$$A_{sp,x} = \frac{N_x / t}{m_x} \text{ (counts} \cdot \text{s}^{-1} \cdot \text{g}^{-1}\text{)}, \quad (2)$$

where  $\theta$  – the abundance of the capturing isotope of the element of interest;  $I$  – the number of  $\gamma$ -rays emitted per capture;  $M$  – the atomic weight,  $\sigma$  ( $E_\gamma$ ) the capture cross-section for neutron energy  $E_\gamma$  while  $\epsilon$  ( $E_\gamma$ ) is the counting efficiency (full energy or double-escape peak) of the detector at energy  $E_\gamma$ .

It has been assumed that, for nearly all elements at neutron energies less than 5 MeV, the neutron cross section ( $\sigma$ ) is inversely proportional to velocity  $v$ , hence  $\sigma = \sigma_0 \cdot v_0/v$ , where  $v_0$  is the standard velocity of thermal neutron (2200 m/s) [4]. Following the convention used in neutron activation analysis as defined by [13]:

$$C_x = \frac{A_{sp,x}}{A_{sp,c}} \cdot \frac{1}{k_{0,c}(x)} \cdot \frac{\epsilon_c}{\epsilon_x} \text{ ppm}, \quad (3)$$

where,  $C_x$  – the concentration of the matrix element under consideration;  $A_{sp}$  – the count rate per unit weight of the elemental sample  $x$  and comparator  $c$ . The indexes “ $x$ ” and “ $C$ ” stand for the analyte and the co-irradiated chlorine comparator,  $k_{0,c}$  is the  $k_0$  factor and  $\epsilon$  is the relative  $\gamma$ -ray efficiency of the elemental sample  $\epsilon_x$  and comparator  $\epsilon_c$ .

The  $k_0$ -prompt  $\gamma$ -factors for the majority of the elements that can be determined via PGAA were experimentally measured with a high accuracy and were tabulated [6 - 8]. The only difference with respect to NAA is that no saturation, decay and counting correction factors appear in the prompt case. However, in Eq. (3), the weights of element ( $x$ ) and sample are expressed in  $\mu\text{g}$  and gram, respectively, so that  $C_x$  is in  $\mu\text{g/g}$ .

## Experimental

### Samples Preparation

Ten short sediment and aqueous core samples were recovered manually in the El-Manzala lagoon, i.e. the core samples were collected at 3 - 5 cm interval and placed into well-numbered plastic bags. Sediment description was also made while sampling. After removing extraneous materials, the collected samples were air-dried in the laboratory at room temperature and then oven-dried at 105 °C until they reached constant mass. The samples were ground, sieved to 200 mesh and prepared for prompt  $\gamma$ -neutron activation analysis, (10 g) of sediment samples was weighed into a PTFE beaker and 500 ml of 70 %  $\text{HClO}_4$  (Merck, Darmstadt,

Germany) and 100 ml of 48 %  $\text{HF}$  (Merck) were added. The sample was heated in a sand bath to incipient dryness. The acid attack with  $\text{HClO}_4$  and  $\text{HF}$  (1 + 2) was repeated three times to complete digestion of the silicate matrix. Then the samples were transferred into flasks and diluted with 0.2 %  $\text{HCl}$ . In most of the cases, chloride compounds of the element were used. Wherever specific stoichiometric chloride compounds are not available, the elements of interest in their stoichiometric compound or metallic forms were mixed with high pure  $\text{NH}_4\text{Cl}$  served as the internal monostandard comparator. The simplest way to ensure the accurate mass ratio of two components in the sample is the usage of stoichiometric compounds. Most of the chemicals had the purity of 99.9 - 99.99 %.

### AC-PGAA System and Detectors

Prompt  $\gamma$ -rays emitted from investigated samples due to thermal neutron captured and then, the binding energy of the neutron is emitted promptly in the form of  $\gamma$ -radiation. This radiation is characteristic, in that the energies of the  $\gamma$ -photons are specific to the nucleus, while their numbers are proportional to the quantity of that nuclide. By analyzing the energy spectrum of the emitted prompt  $\gamma$ -radiation, the isotopic and elemental contents of the irradiated sample can be determined [5].

The basic instrument of the PGAA facility consists of a p-type high-purity germanium (HPGe). A schematic drawing of the HPGe-NaI(Tl) schematic of electronic system and detector assembly is shown in Figs. 1 and 2.

The Compton-suppressed detector system consists of a HPGe main detector (Canberra) and a NaI(Tl) surrounding the main detector, and is known as a surrounding shield “guard”. The system has a peak-to-Compton ratio of about 350:1 for  $^{60}\text{Co}$ . The signals are processed with standard NIM electronics, and the spectra are collected into 16 thousand channels by a Canberra S100 multichannel analyzer. Typical normal and Compton-suppressed spectra are shown in Fig. 3.

A  $^{252}\text{Cf}$  neutron source of neutron flux of  $6.16 \cdot 10^6 \text{ n} \cdot \text{cm}^{-2} \cdot \text{sec}^{-1}$  is located inside cubic paraffin blocks in irradiation position and the detection system consists of an HPGe detector of 25 % efficiency with 1.95 keV resolution capabilities FWHM at 1332 keV of  $^{60}\text{Co}$ . The signals from the detector were passed after suitable amplification to (a 16 k channel) multichannel analyzer and using the software Genie-2000 used for data acquisition and analyses. The absolute energy calibration of the detector for low energy range up to 2000 keV was established using the  $\gamma$ -lines of standard sources  $^{137}\text{Cs}$  (662 keV),  $^{60}\text{Co}$  (1173 and 1332 keV).

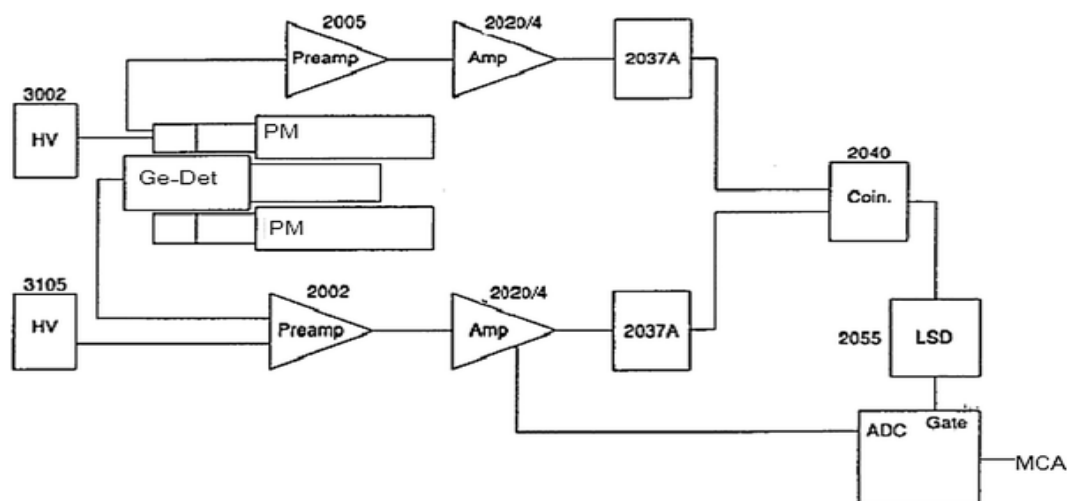


Fig. 1. Block diagram of the electronics set-up in anticoincidence mode.

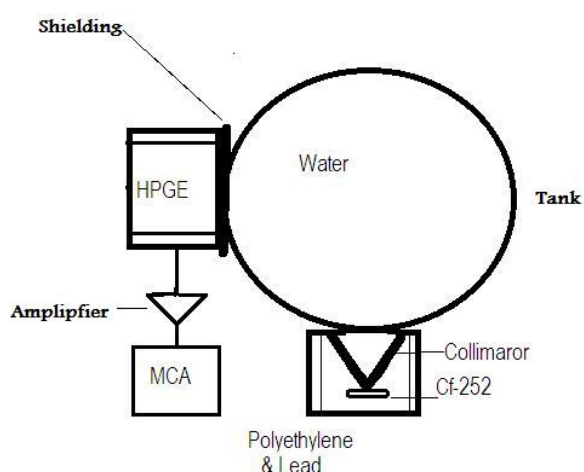


Fig. 2. A sketch showing the  $^{252}\text{Cf}$  neutron source – target position.

To reduce the neutron dose in the detector, the latter is surrounded by 2.5 cm thick hollow cylinder made of borated polyethylene and a fused  $\text{Li}_2\text{CO}_3$  (with  $^6\text{Li}$ ) block of 1.5 cm thickness is placed in front of the detector.

For relative efficiency calibration, the emission probabilities of the  $\gamma$ -rays from  $^{152}\text{Eu}$ ,  $^{35}\text{Cl}$ ,  $^{48}\text{Ti}$  and the three energy peaks of hydrogen from the measured background spectrum were taken from previously reported data [6 - 8]. These peaks are, the full energy line 2223.1 keV, the single escape line at 1712.1 keV and the double escape line at 1201.1 keV arising from the pair production process of the full energy prompt  $\gamma$ -line of hydrogen with the HPGe detector [8].

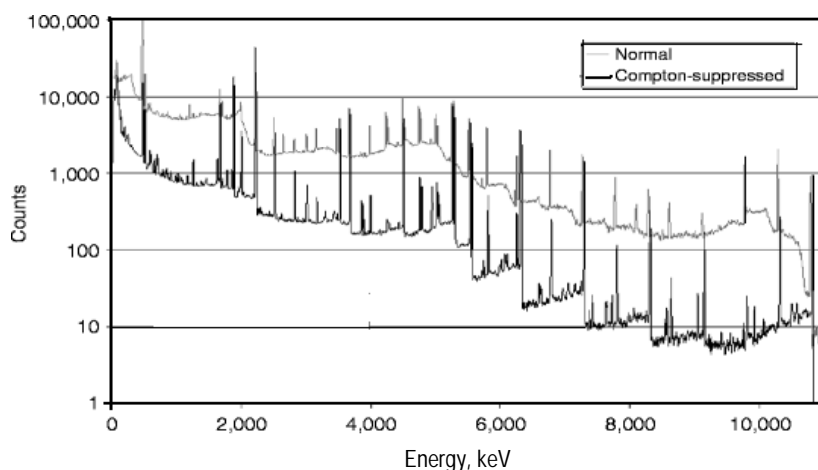


Fig. 3. Normal and Compton-suppressed spectra of a nitrogen-containing compound (high density polyethylene).

The calibration fitting PGAA measurements were carried out using a thermal neutron beam. The average neutron flux at the sample positions, defined for the exact neutron spectrum, was  $6.16 \cdot 10^6 \text{ n}/(\text{cm}^2 \cdot \text{s})$ , and the cadmium ratio (using two gold foils, one of them cadmium covered) is 160. The PGAA spectra were measured for 50000 to

70000 s. The HPGe detector was used for counting prompt  $\gamma$ -rays. The resolution of the detector was 1.9 and 1332 keV of  $^{60}\text{Co}$ . The MCA was calibrated in the region of 0.121 to 8 MeV using delayed  $\gamma$ -rays from  $^{152}\text{Eu}$  and prompt  $\gamma$ -rays from Cl.

The prompt  $\gamma$ -ray peak at 1951.1 keV was used to determine the internal monostandard Cl. The

isotopic cross section of  $^{35}\text{Cl}$  is 43.6 barn. The isotopic abundance of  $^{35}\text{Cl}$  is 75.78 % and of  $^{37}\text{Cl}$  24.22 %. Chlorine has an elemental cross section of 33.1 barn. The prominent neutron induced prompt  $\gamma$ -ray energies of chlorine were 516.7, 788.4, 1164.8, 1951.14, 6110.8 and 7413.9 keV. A mixture of 2 gm ( $\text{NH}_4\text{Cl}$ ) and unknown sample was used in the study.

## Results and discussion

### Monte Carlo simulation

The Monte Carlo simulations of neutron transport were performed with the code MCNP version 5 using the cross section data library JEF 2.2 [14]. The schematic of a typical MCNP run is shown in Fig. 2.

It consists of a cylindrical tank of polyethylene containing the 0.125 m<sup>3</sup> volume of water irradiated by neutrons emitted from a  $^{252}\text{Cf}$  source. The code was set up to generate on a three-dimensional geometry with the mode card n the neutrons flux distribution, resulting from the nuclear interaction of neutron inside water sample. Thermal Neutron flux distribution using point detector (F5: N tally) and neutron flux average over water cell, track length estimate (F4: N tally) were calculated in units of cm<sup>-2</sup> per neutron. Relative thermal neutron flux variation versus the depth across central axis of water is plotted in Fig. 4. The relative errors of the computation were kept within the statistical uncertainty 5 - 11 %.

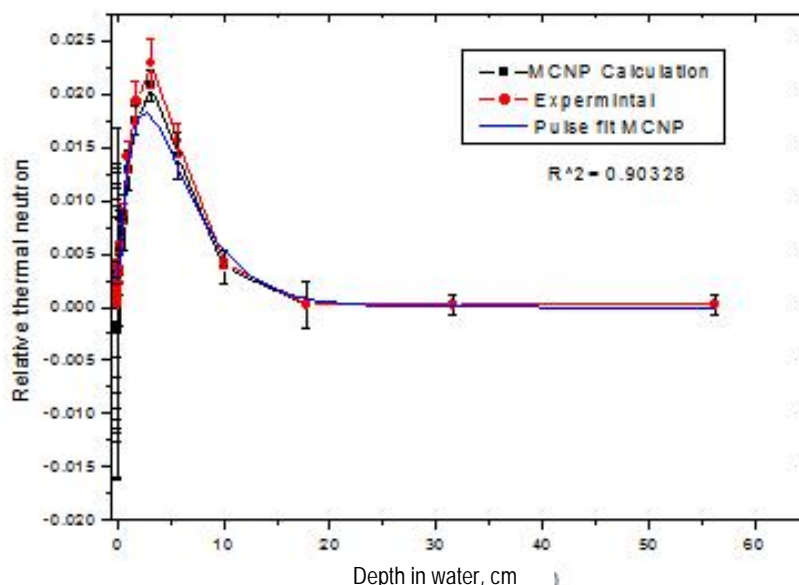


Fig. 4. Relative thermal neutron fluency versus depth along the central axis of aqueous solution sample.

### Flux calculations

MCNP was run until generated 1E6 histories on neutrons mode only for both thermal neutron distribution and track length estimate tallies. The various values obtained for flux distribution curve were adjusted by a non-linear curve fitting called "Pulse" function. Hydrogen plays a very essential role in thermalization of neutrons. The most intense value of the neutron flux was ( $10^6$  n/(cm<sup>2</sup> · s) which correspond to depth of 4.3 cm in the central axis of water.

The increased hydrogen concentration causes higher levels of thermal flux closer to the neutron source. At 20 cm from the  $^{252}\text{Cf}$  source 77 % of the total flux was reached, while 92 % of the neutron irradiation into water tank was confined within 40 cm. This result confirms the choice of the optimum volume of water (49 cm of the diameter) used in this work.

Thermal neutron flux measurement using  $\text{BF}_3$

proportional counter were performed in order to verify that the radiation safety requirements are satisfied (2.5 mRem/h at 3 m distance from the source) and to extend the calculations of thermal neutron flux just outside water tank. The values obtained (less than 1 n/(cm<sup>2</sup> · s) agreed with MCNP calculations.

The average neutron flux inside the water was  $10^5$  n/(cm<sup>2</sup> · s), the value obtained using MCNP code and track length estimate tally.

### Detector Efficiency calibration

The detector efficiency for this geometry was deduced by irradiating 0.125 m<sup>3</sup> volume of water in which 13 g/l of  $\text{NH}_4\text{Cl}$  was dissolved. Thermal neutron capture of chlorine has a cross section as high as 33.1 barns and it provides a series of high energy  $\gamma$ -rays spanning a wide energy range commonly used in PGNAA. The prompt  $\gamma$ -spectrum was counted for 7200 s and efficiency at different

energies was determined using the area photo-peaks over  $\gamma$ -ray intensities and the average value of the thermal flux. For comparison, the detector efficiency was also calculated for voluminous source such as tank of water. This was done using the Monte Carlo program, which calculates the absolute efficiency of a voluminous source considering the  $\gamma$ -rays attenuation within the sample, the detector material and any shielding material. The physical dimensions of the detector were supplied by the manufacturer. Thus the total efficiency is expressed as:

$$\ln \varepsilon_E = K_j + \sum_{i=0}^m a_i (\ln E)^i, \quad (4)$$

where,  $\varepsilon$  – the full energy peak detection efficiency of  $\gamma$ -ray of energy  $E$ ,  $k_j$  is a constant characteristic of the  $j^{\text{th}}$  nuclide and  $m$  is the order of the polynomial that can be chosen depending on the energy range of interest.

In Table 1 the  $\gamma$ -ray yields from  $^{35}\text{Cl}(n, \gamma)^{36}\text{Cl}$  thermal neutron reaction where, MCA was calibrated in the region of 0.1 to 10 MeV using prompt  $\gamma$ -rays from Cl. The prompt  $\gamma$ -ray peak at

1951.1 keV was used to determine the comparator Cl [8].

Table 1.  $\gamma$ -ray yields from  $^{35}\text{Cl}(n, \gamma)^{36}\text{Cl}$  thermal neutron reaction [8]

E, keV	Intensity, %
1950.9	21.72
6110.9	20
1164.7	19.93
516.7	18.5
788.4	15
1959.1	14.62
7413.8	10.42
786.3	9.6
7790.2	8.55
6619.5	8.01
2860.9	6.93
5715.26	5.5
6627.64	4.54
1600.8	4.16
1162.6	1.3

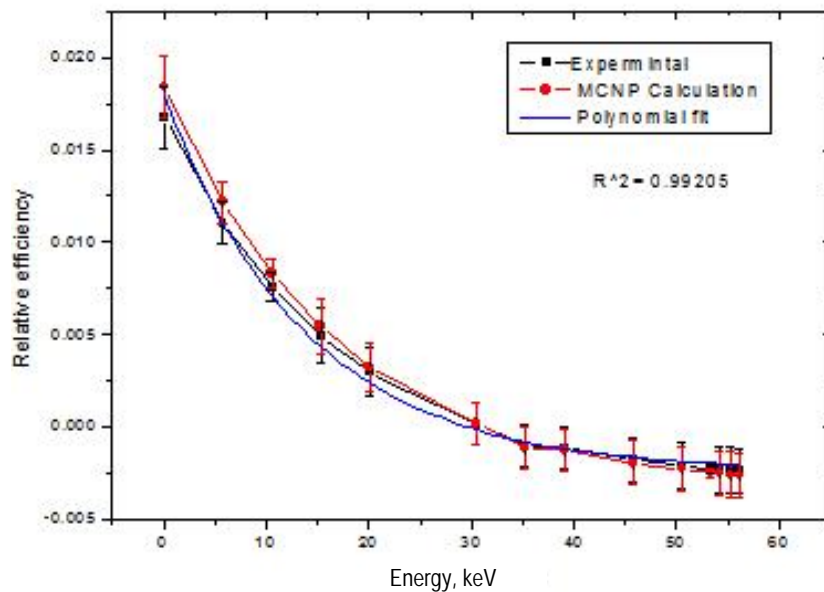


Fig. 5. Relative efficiency versus energy ( $R$  is the coefficient of correlation of the polynomial fit).

The relative detector efficiency versus  $\gamma$ -rays energy was plotted in Fig. 5, where the various values obtained were fitted with a polynomial curve. All simulations in this study were done using MCNP. The code simulations are normalized to  $10^6$  source particles ( $nps = 10^6$ ). The desired result in the simulation component of this study is a pulse height spectrum since it produces the distribution of the energy deposited in a cell, i.e. the  $\gamma$ -ray energy spectrum in a physical model of a detector. Pulse height spectra simulations are obtained in MCNP

using f8 tally. The variation of the relative efficiency was significant at the energies lower than 4000 keV. The reliability of the flux calculation with MCNP code used in this work has been checked, and acceptable agreement between measured and calculated detector efficiency has been observed.

#### Quality Control and Validation of the $k_0$ -PGAA

Validation of the results was achieved by applying the method performed by using the reference material IAEA Soil-7. The analytical

results given in Table 2 are based on the measurements of sample with mass of 20 g, with duration of about 24 h. The certified value of the most abundant element, namely Si in both reference material and samples, has been used for normalization to obtain absolute concentrations. The result obtained agreed with the certified values within one combined standard deviation ( $1\sigma$ ).

**Table 2. Determined concentrations of IAEA Soil-7 for the comparative and the k<sub>0</sub>-methods, using the <sup>35</sup>Cl as a comparator**

Product element	Average concentration values, $\mu\text{g/g}$	Reported concentration, $\mu\text{g/g}$ [10]
Na (%)	$0.24 \pm 0.10$	$0.25 \pm 0.1$
Mg (%)	$2.13 \pm 0.05$	$2.25 \pm 0.1$
Al (%)	$4.70 \pm 0.4$	$4.62 \pm 0.07$
Si (%)	$1.80 \pm 0.13$	$1.774 \pm 0.17$
p	$459.0 \pm 0.39$	$460.0 \pm 0.39$
K (%)	$1.21 \pm 0.13$	$1.174 \pm 0.17$
Ca (%)	$0.3 \pm 0.07$	$0.25 \pm 0.07$
Ti (%)	$0.03 \pm 0.13$	$0.034 \pm 0.17$
V	$66.0 \pm 7.00$	$68.7 \pm 1.9$
Mn	$631.0 \pm 18.90$	$540.2 \pm 16.7$
Fe (%)	$2.57 \pm 0.13$	$2.574 \pm 0.17$
Co	$8.8 \pm 1.20$	$8.9 \pm 1.00$
Zn	$239.0 \pm 12.00$	(-)
La	ND	$28.1 \pm 1.00$
Rb	$54.0 \pm 14.00$	$55.0 \pm 14.00$
Cd	$3.41 \pm 0.07$	$1.3 \pm 0.07$
Sm	$5.5 \pm 12$	$5.1 \pm 9.0$
Gd	$6.82 \pm 1.73$	(-)

(-) Not reported; ND: Not detected; (%): percentage.

#### Sediment and aqueous Samples location

Manzala Lake is considered as the most polluted area of all Egyptian Lakes. Its length is about 190 km and extends from south of Cairo, passing by the provinces of Qalyoubeya East, Ismailia and Dakahlia

and empties into Manzala lake. The lake continues to receive sediment, nutrients and other types of pollutants from runoff from the surrounding farmlands and cities. In recent years it has attracted much attention of environmentalists because of the highly polluted status at several points. Baher El Baqar lagoon has identified around 27 cities and 120 factories as points of pollution from provinces Cairo to Port-Said (in east northern of Egypt). Cairo is a major industrial city with over 200 tanneries and about 40 million populations where treated or untreated effluents are directly discharged into the Lake. Therefore, several heavy metal pollutants, particularly Mn, Cr, Cd and Zn enter into the river thus polluting the entire water stream.

A perusal of data in Table 3 with statistical uncertainty of  $\pm 1$  to 4 %, shows that Cr, Mn, Cd and Zn concentrations in both the surface and subsurface sediments and aqueous samples in Bahr El-Baqar bottom- I are higher compared to similar samples in Gayara Island. This is primarily due to the fact that the metals from tannery effluents and other industries are being deposited heavily at down streams in Bahr El-Baqar bottom-I.

The Fe contents also follow a similar trend for subsurface sediments and aqueous samples but for the surface sediments it is more at Gayara Island than at Bahr El-Baqar bottom-I. Here it may be noted that the aquatic environment is contaminated with heavy metals, especially chromium, in tannery areas, as chrome liquor is extensively used in tanneries and the waste discharged into the Lake.

Based on these observations it can be emphasized that effluents from tanneries severely affect the aquatic environment by contaminating the Lake water chromium and other heavy metals. Besides, several other studies have also reported contamination of ground and/or river water by Cr, Mn, Zn, Hg, Cd and Pb and other pollutants due to tannery and other industries effluents [11, 12].

**Table 3. Results of multi-elemental analysis in surface and subsurface sediments of El-Manzala Lake**

Element, ppm	Gayara Island		Bahr El-Baqar bottom-I	
	Surface	Subsurface	Surface	Subsurface
Cd	$3.72 \pm 0.2144$	$3.36 \pm 0.2708$	$3.77 \pm 0.536$	$3.4 \pm 0.2688$
Co	$6.72 \pm 0.2688$	$5.36 \pm 0.2144$	$6.77 \pm 0.2708$	$13.4 \pm 0.536$
Cr	$33.7 \pm 1.348$	$17.2 \pm 0.688$	$103 \pm 4.12$	$59.5 \pm 2.38$
Cs	$6.49 \pm 0.2596$	$4.4 \pm 0.176$	$4.67 \pm 0.1868$	$7.35 \pm 0.294$
Fe (mg/g)	$28.7 \pm 1.148$	$17.1 \pm 0.684$	$18.7 \pm 0.748$	$37.5 \pm 1.5$
Hg	$29.7 \pm 1.188$	$58 \pm 2.32$	$9.09 \pm 0.3636$	$40.4 \pm 1.616$
K (mg/g)	$11.7 \pm 0.468$	$14.4 \pm 0.576$	$18.3 \pm 0.732$	$17.8 \pm 0.712$
La	$50.9 \pm 2.036$	$49.5 \pm 1.98$	$42.7 \pm 1.708$	$26.6 \pm 1.064$
Mn	$379 \pm 15.16$	$318 \pm 12.72$	$424 \pm 16.96$	$362 \pm 14.48$

Element, ppm	Gayara Island		Bahr El-Baqar bottom-I	
	Surface	Subsurface	Surface	Subsurface
Na (mg/g)	8.88 ± 0.3552	9.76 ± 0.3904	8.85 ± 0.354	8.15 ± 0.326
Rb	114 ± 4.56	47.4 ± 1.896	32.7 ± 1.308	119 ± 4.76
Sc	9.2 ± 0.368	6.25 ± 0.25	6.44 ± 0.2576	1.32 ± 0.0528
Th	35.6 ± 1.424	25.4 ± 1.016	7.44 ± 0.2976	1.62 ± 0.0648
Zn	88.2 ± 3.528	65.1 ± 2.604	120 ± 4.8	96.5 ± 3.86

Furthermore, it is observed from Table 3 that Cr, Mn and Zn concentrations in subsurface sediments of Bahr El-Baqar bottom-I are significantly higher compared to those of Gayara Island though these are lower when compared to those in the surface sediments of both sampling sites. It means that these metals are sinking down the surface after they enter into the Lake. Surprisingly Fe, Co, Cs and Rb have not shown any definite trend as these are higher in surface at Gayara Island but lower in Bahr El-Baqar bottom-I. Alkali metals (Na and K) are almost comparable in all the ten samples.

The background spectrum of elements in AC-PGAA system were determined and subtracted from all measuring samples. Those elements appear in the prompt and delayed regions of the  $\gamma$ -spectrum generated from inner High density polyethylene (C, H and O) and outer shielding materials (Fe, Cd, Pb).

The analysis of the spectral shapes has indicated that, in the measuring arrangement the contribution of room scattered neutrons to the (n,  $\gamma$ ) reactions could be neglected.

Due to complication of prompt  $\gamma$ -spectrum which owning delayed  $\gamma$ -spectrum in the same time (Fig. 6). Hence, one can give some examples of nuclear reactions. When taking boron in consideration, the thermal neutron capture cross section 716 barn, based on the nuclear reaction  $^{10}\text{B}(n, \alpha)^7\text{Li}$ . The reaction  $\gamma$ -ray yields 477.595 KeV which could interfere with  $\gamma$ -line 472 keV yield of  $^{22}\text{Na}(n, \gamma)^{23}\text{Na}$ ; the separation of them was not difficult when using detectors with good resolution. With respect to chlorine, the single escape peaks of 6108.5 and 6116.6 keV overlap with the 6110.9 keV full-energy peak, which creates a confusion for the actual count rate of 6110.9 keV.

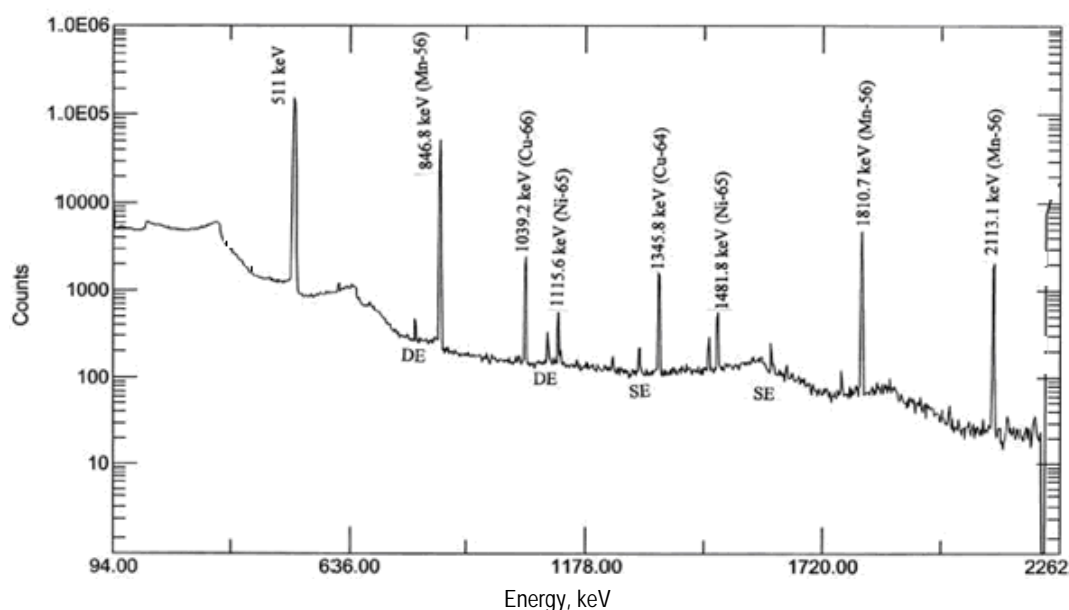


Fig. 6. Portion of  $\gamma$ -ray spectrum of one of the activated sample.

In Table 4, the close doublet of the 788.4 and 786.3 keV thermal neutron capture  $\gamma$ -rays of chlorine have intensities of 15 and 10 %, respectively. The 1164.7 keV peak is also a close doublet with 1162.6 keV. These peaks are very close to each other and thus the assessment of the actual count rate is difficult due to the interference. The separation of 1950.9 and 1959.1 keV was not difficult when using

detectors with 1.02 keV resolution. The prompt  $\gamma$ -rays energies, at 1950.9 keV, were found suitable for the measurement of the count rate.

In case of hydrogen, we have first, single and double escape photo-peaks at 2223.3, 1712.3 and 1201.3 keV, respectively. The peak resulting from the  $^{70}\text{Ge}(n, \gamma)^{71}\text{Ge}$  appears to be small in comparison to the photon peak resulting from the

Table 4. Prompt k<sub>0</sub>-factors of different elements versus the 1951.1 keV  $\gamma$ -rays of <sup>35</sup>Cl and interferences for capture  $\gamma$ -ray important for analysis of various elements

Isotope	Major E <sub><math>\gamma</math></sub> , keV	$\sigma_{\gamma}^*$ (E $\gamma$ )	k <sub>0</sub> [2, 7, 8, 10]	Interference Elements [2, 11]
<sup>2</sup> H	2223.248	0.3326 ± 7.00 · 10 <sup>-4</sup>	1.85 ± 0.214	S, Ge, Ba, Mg, Br
	1712.3 SE	0.3326 ± 7.00 · 10 <sup>-4</sup>		
	1201.3DE	0.3326 ± 7.00 · 10 <sup>-4</sup>		
<sup>11</sup> B	477.595	716 ± 25	372 ± 7.01	Na, K, Sn, Cs, Sm, Yb
<sup>24</sup> Na	472.209D	0.478 ± 10 <sup>-2</sup>	0.063 ± 1.71E-3	K, Sn, Cs, Sm, Yb
	869.2	0.108 ± 1.3 · 10 <sup>-3</sup>	2.622 · 10 <sup>-2</sup> ± 1.71 · 10 <sup>-4</sup>	Gd
	1368.66D	0.53 ± 0.05	1.29 · 10 <sup>-1</sup> ± 2.3 · 10 <sup>-2</sup>	Sr, Gd
<sup>25</sup> Mg	585.0	0.0314 ± 11 · 10 <sup>-2</sup>	7.25 · 10 <sup>-3</sup> ± 1.37 · 10 <sup>-4</sup>	Sr, Tb, Tm, Re, As
<sup>26</sup> Mg	1808.7	0.018 ± 5 · 10 <sup>-2</sup>	4.14 · 10 <sup>-3</sup> ± 6.37 · 10 <sup>-5</sup>	P, Cl, Co
<sup>28</sup> Al	1778.92D	0.231 ± 3 · 10 <sup>-2</sup>	4.82 · 10 <sup>-2</sup> ± 9.5 · 10 <sup>-3</sup>	Sc, V,
	7724	0.0493 ± 1.5 · 10 <sup>-3</sup>	1.02 · 10 <sup>-2</sup> ± 1.68 · 10 <sup>-4</sup>	N, F
<sup>29</sup> Si	1273.349	0.0289 ± 6 · 10 <sup>-4</sup>	5.77 · 10 <sup>-3</sup> ± 5.77 · 10 <sup>-3</sup>	Nb, Hg
	4933.9	0.1120 ± 2.3 · 10 <sup>-3</sup>	2.24 · 10 <sup>-2</sup> ± 2.48 · 10 <sup>-4</sup>	Mn
<sup>32</sup> P	636.663	0.0311 ± 4.4 · 10 <sup>-3</sup>	5.62 · 10 <sup>-3</sup> ± 1.3 · 10 <sup>-4</sup>	Cl, Gd
<sup>33</sup> S	841.91D	0.00408 ± 1.2 · 10 <sup>-4</sup>	6.074 · 10 <sup>-2</sup> ± 1.3 · 10 <sup>-4</sup>	Yb, Eu, Gd
<sup>34</sup> S	2379.661	2.08 · 10 <sup>-1</sup> ± 5 · 10 <sup>-2</sup>	0.0365 ± 1.3 · 10 <sup>-2</sup>	Zn
<sup>33</sup> S	3220.588	1.17 · 10 <sup>-1</sup> ± 2.3 · 10 <sup>-6</sup>	2.056 · 10 <sup>-2</sup> ± 2.17 · 10 <sup>-7</sup>	F, U
<sup>36</sup> Cl	517.1	7.58 ± 5 · 10 <sup>-2</sup>	1.2 ± 4.27 · 10 <sup>-3</sup>	Ar, Ge, Au, Ba
	786.3	3.42 ± 3 · 10 <sup>-3</sup>	0.541 ± 0.74 · 10 <sup>-2</sup>	Au, Ge, La, W
	788.43	5.42 ± 0.05	0.856 ± 0.427 · 10 <sup>-2</sup>	Au, Ge, La, W
	1164.87	8.91 ± 0.04	1.41 ± 3.2 · 10 <sup>-3</sup>	Cs, Au, Th
<sup>40</sup> K	770.305	0.903 ± 1.2 · 10 <sup>-2</sup>	1.29 · 10 <sup>-1</sup> ± 2.71 · 10 <sup>-1</sup>	Sm, Gd, S, Ge
<sup>41</sup> Ca	1942.67	0.352 ± 7 · 10 <sup>-3</sup>	4.9 · 10 <sup>-2</sup> ± 1.5 · 10 <sup>-1</sup>	Er
<sup>57</sup> Fe	352.347	0.273 ± 0.03	0.0274 ± 1.63 · 10 <sup>-2</sup>	As, Dy, Tb, W, Tm, Os, Rh
<sup>60</sup> Co	277.161	6.77 ± 0.08	0.643 ± 4.11 · 10 <sup>-3</sup>	Gd, Cu
<sup>64</sup> Cu	278.25	0.893 ± 0.0145	7.87 · 10 <sup>-2</sup> ± 7.15 · 10 <sup>-2</sup>	Gd
<sup>76</sup> As	165.05	0.996 ± 16 · 10 <sup>-2</sup>	7.445 · 10 <sup>-2</sup> ± 6.74 · 10 <sup>-2</sup>	Rh, Nd
<sup>80</sup> Br	195.602	0.434 ± 0.14	3.05 · 10 <sup>-2</sup> ± 5.31 · 10 <sup>-2</sup>	Co, Ag, Ti, Lu
<sup>114</sup> Cd	558.3	1860 ± 30	92.926 ± 0.89	Sm, F
	651.19	358 ± 0.05	17.7 ± 0.135	Fe
<sup>139</sup> Ba	165.9D	0.074.8 ± 0.09	3.02 · 10 <sup>-3</sup> ± 21 · 10 <sup>-4</sup>	Gd
	2217.84	0.044 ± 2.00 · 10 <sup>-5</sup>	0.0468 ± 0.1	H
<sup>150</sup> Sm	333.97	4790 ± 60	179 ± 1.21	Fe, K, Cl
<sup>158</sup> Gd	182	7200 ± 300	257 ± 5.78	Dy
	944.17	3090 ± 70	110 ± 1.35	Cl, Sm, Al

\* – Thermal neutron capture; D = Decay  $\gamma$ , SE – Single escape; DE – Double escape.

<sup>1</sup>H(n,  $\gamma$ )<sup>2</sup>H reaction. However the spectral interference should be taken into account for all subsequent H analysis. It should also be noted that the ratio of counts produced from the <sup>70</sup>Ge(n,  $\gamma$ )<sup>71</sup>Ge reaction is higher than the counts produced in the <sup>73</sup>Ge(n,  $\gamma$ )<sup>74</sup>Ge reaction indicating that the reactions observed in the detector background count result from fast neutron interactions. In magnesium, the most appropriate reaction for detecting this element is <sup>23</sup>Mg(n,  $\gamma$ )<sup>24</sup>Mg (E <sub>$\gamma$</sub>  = 1808.668 keV), and the possible interference produced via <sup>58</sup>Co(n,  $\gamma$ )<sup>59</sup>Co at E = 1808.82 keV and <sup>139</sup>Ce(n,  $\gamma$ )<sup>140</sup>Ce at E <sub>$\gamma$</sub>  = 1808.67 keV were considered with a necessary correction. At E <sub>$\gamma$</sub>  ≈ 4940 keV there is an obvious overlap between the two  $\gamma$ -lines (4934 and 4945 keV) resulting from the <sup>28</sup>Si(n,  $\gamma$ )<sup>29</sup>Si reaction

and the <sup>12</sup>C(n,  $\gamma$ )<sup>13</sup>C reaction respectively. Additionally, special care has to be devoted to differentiate between the  $\gamma$ -lines attributed to S, K and Gd that closed to each other.

#### Self shielding

However, element sensitivities depend strongly on the geometry and the composition of the sample. Indeed, self-shielding occurs in samples containing large amounts of neutron absorber nuclides (B, Cd, Eu, Gd, ... etc.) resulting in lower element sensitivities. Furthermore, an increase or decrease in elemental sensitivities, depending on the sample geometry, ensues from large concentrations of neutron scattering nuclides (hydrogen particularly).

These analytical biases disappear in homogenous

samples if elemental ratios are determined. The ratio of the experimentally measured sensitivity for a studied element to that of an internal standard is independent of sample geometry or composition [13].

### Conclusion

In conclusion, the AC-PGAA system facility consisting of  $^{252}\text{Cf}$  neutron source can be used as a radio analytical tool for determining the presence and quantity of elements in sediment samples by irradiating them continuously with neutrons. The presence of a number of peaks from each element has made possible relatively low uncertainties for the final results as all of these peaks and their ratios with each other are unchanged from the pure element that can be used in the analysis. Matrix effects and sample self shielding have been in consideration and the resultant corrections were found to be small or neglected.

Higher concentrations of some of the elements viz. Cr, Mn and Zn in sediment samples collected from the Manzala Lake at Bahr El-Baqar bottom-I site compared to those from Gayara Island can be attributed to the mixing up of effluents from tanneries and other industries located around the site. Cr originating from tannery waste exhibits downward movement and is preferentially absorbed by the sediments, thus polluting Manzala Lake.

The River Nile delta lakes receive huge amounts of different contaminants; especially trace metals in El-Manzala Lake. The uncontrolled discharge of untreated sewage, industrial and agricultural wastes is the cause for enriching these contaminants at the sediments of the lake particularly in the vicinity of the discharge points.

Finally this technique could be used as a movable instrument in several open fields like detection and disposal of explosive ordnance and unexploded ordnance land mines.

### REFERENCES

1. *Molnár G.L., Lindstrom R.M.* Nuclear reaction prompt  $\gamma$ -ray analysis // Nuclear Techniques in Mineralogy and Geology / Ed. by A. Vértes, S. Nagy, K. Süveg. - New York: Plenum Publishing, 1998. - P. 145 - 164.
2. *Molnár G.L., Révay Zs., Belgya T., Firestone R.B.* The new prompt  $\gamma$ -ray catalogue for PGAA // Appl. Radiat. Isot. - 2000. - Vol. 53. - P. 527 - 533.
3. *Darwish Al-Azmi.* Simplified slow anti-coincidence circuit for Compton suppression systems // Applied Radiation and Isotopes. - 2008. - Vol. 66, Issue 8. - P. 1108 - 1116.
4. *Molnar G.L., Reveay Zs., Paul R.L., Lindstorm R.M.* Prompt  $\gamma$ -Activation Analysis Using the  $k_0$  Approach // J. Radioanal. Nucl. Chem. - 1998. - Vol. 234. - P. 21.
5. *Hassan M., Gantner E., Mainka E. et al.* Analytical applications of neutron capture  $\gamma$ -ray spectroscopy // KFK 3387 Karlsruhe: Kernforschungszentrum, 1982.
6. *Reddy R.C., Frankle S.C.* // At. Data Tables. - 2002. - Vol. 80. - P. 1 (<http://www-nds.iaea.org/pgaa/>).
7. *IAEA-TECDOC-619* // X-ray and G-ray Standards for Detector Calibration. - Vienna: IAEA, 1991.
8. *IAEA-TECDOC (Draft)* // Database of Prompt  $\gamma$ -rays from Slow Neutron Capture for Elemental Analysis. - Vienna: IAEA, 2010.
9. *Firestone R.B.* // Table of Isotopes / Eighth ed. - USA: Wiley, 1996.
10. *Pszonicki L.* Report on Intercomparison IAEA, Soil-7 of the Determination of Trace Element in Soil // IAEA/RL/112, Austria, 1984.
11. *Osfor M.M., el-Dessouky S.A., el-Sayed A., Higazy R.A.* Relationship between environmental pollution in Manzala Lake and health profile of fishermen // Nahrung. - 1998. - 42(1):42-5. PubMed PMID: 9584278.
12. *Adel A. Ramadan* Heavy Metal Pollution and Biomonitoring Plants in Lake Manzala, Egypt // Pakistan Journal of Biological Sciences. - 2003. - Vol. 6(13). - P. 1108 - 1117.
13. *Hamid A.*  $k_0$ -prompt  $\gamma$ -ray activation analysis for estimation of boron and cadmium in aqueous solutions // J. Radioanal. Nucl. Chem. - 2012. - Vol. 292(1). - P. 229 - 236.
14. *Briesmeister J.F.* MCNP - a general Monte Carlo N-particles transport code, version 4c // Technical Report LA-13709, Los Alamos National Laboratory, USA, 2000.

Ашраф Хамід<sup>1</sup>, Хешам Шахбандер<sup>2</sup>

<sup>1</sup> Департамент радіоактивного забруднення навколишнього середовища, Центр "Hot Laboratories",  
Управління атомної енергії, Каїр, Єгипет

<sup>2</sup> Університет "Айн Шамс", фізичний факультет, факультет природничих наук, Каїр, Єгипет

### **$k_0$ -НЕЙТРОННИЙ АКТИВАЦІЙНИЙ АНАЛІЗ ВМІСТУ ЗАБРУДНЮЮЧИХ РЕЧОВИН У ВОДНИХ ВІЗКАХ ІЗ ВИКОРИСТАННЯМ ПРОГРАМИ MCNP**

Розглянуто швидкий активаційний аналіз (PGNAA) з використанням методу  $k_0$  по  $\gamma$ -лінії 1951,1 кеВ реакції  $^{35}\text{Cl}(n, \gamma)^{36}\text{Cl}$  на теплових нейтронах як стандартного компаратора. Метод було застосовано та перевірено за допомогою антикомптонової установки для швидкого  $\gamma$ -нейтронного активаційного аналізу з використанням джерела нейтронів  $^{252}\text{Cf}$  з потоком нейтронів  $6,16 \cdot 10^6 \text{ н} \cdot \text{см}^{-2} \cdot \text{с}^{-1}$ . Добре відомий HPGe детектор в якості

основного детектора, оточений NaI(Tl) детектором, було встановлено для дослідження ефективності комптонівського спектрометра за спрощеною повільною схемою. Властивості потоку нейтронів визначалися з розрахунків за програмою MCNP. Для знаходження кривої ефективності HPGe детектора використовувалося  $\gamma$ -випромінювання хлору й експериментальні дані підганялись експоненціальною залежністю. Метод АС-PGNAA було використано для визначення як сильно поглинаючих нейтрони елементів, таких як Cd, Sm та Gd, а також і 20 легких та важких елементів (Na, Mg, Al, Si, P, K, Ca, Ti, V, Mn, Sc, Fe, Co, Zn, La, Rb, Cs, As та Th) стандартних еталонних матеріалів (МАГАТЕ, Soil-7) і 10 проб донних відкладень, узятих з озера Ель-Манзала в північній частині Єгипту. Еталонні матеріали МАГАТЕ, Soil-7 було проаналізовано для перевірки даних і було одержано добре узгодження між експериментальними та сертифікованими величинами.

*Ключові слова:* k<sub>0</sub>-PGNAA, АС-PGNAA, джерело нейтронів <sup>252</sup>Cf, забруднення води, програма MCNP, самоекранування.

**Ашраф Хамид<sup>1</sup>, Хешам Шахбандер<sup>2</sup>**

<sup>1</sup> *Департамент радиоактивного загрязнения окружающей среды, Центр "Hot Laboratories",  
Управления атомной энергии, Каир, Египет*

<sup>2</sup> *Университет "Айн Шамс", физический факультет, факультет естественных наук, Каир, Египет*

### **к<sub>0</sub>-НЕЙТРОННЫЙ АКТИВАЦИОННЫЙ АНАЛИЗ СОДЕРЖАНИЯ ЗАГРЯЗНЯЮЩИХ ВЕЩЕСТВ В ВОДНЫХ ОБРАЗЦАХ С ИСПОЛЬЗОВАНИЕМ ПРОГРАММЫ MCNP**

Рассматривается быстрый активационный анализ (PGNAA) с использованием метода k<sub>0</sub> по  $\gamma$ -линии 1951,1 кэВ реакции <sup>35</sup>Cl (n,  $\gamma$ )<sup>36</sup>Cl на тепловых нейтронах как стандартного компаратора. Метод был применен и проверен с помощью антикомptonовской установки для быстрого  $\gamma$ -нейтронного активационного анализа с использованием источника нейтронов <sup>252</sup>Cf с потоком нейтронов  $6,16 \cdot 10^6$  н · см<sup>-2</sup> · с<sup>-1</sup>. Хорошо известный HPGe детектор в качестве основного детектора, окруженный NaI(Tl) детектором, был установлен для исследования эффективности комптонвского спектрометра по упрощенной медленной схеме. Свойства потока нейтронов определялись из расчетов по программе MCNP. Для определения кривой эффективности HPGe детектора использовались  $\gamma$ -лучи хлора и экспериментальные данные подгонялись экспоненциальной зависимостью. Метод АС-PGNAA был использован для определения как сильно поглощающих нейтроны элементов, таких как Cd, Sm и Gd, а также и 20 легких и тяжелых элементов (Na, Mg, Al, Si, P, K, Ca, Ti, V, Mn, Sc, Fe, Co, Zn, La, Rb, Cs, As и Th) стандартных эталонных материалов (МАГАТЭ, Soil-7) и 10 проб донных отложений, взятых из озера Манзала в северной части Египта. Эталонные материалы МАГАТЭ, Soil-7 были проанализированы для проверки данных и было получено хорошее согласие между экспериментальными и сертифицированными величинами.

*Ключевые слова:* k<sub>0</sub>-PGNAA, АС-PGNAA, источник нейтронов <sup>252</sup>Cf, загрязнение воды, программа MCNP, самоэкранирование.

Надійшла 18.11.2013

Received 18.11.2013